










Staphylococcus aureus biofilm properties and chronic rhinosinusitis severity scores correlate positively with total CD4⁺ T-cell frequencies and inversely with its Th1, Th17 and regulatory cell frequencies

Gohar Shaghayegh^{1,2,3}  | Clare Cooksley^{1,2,3}  | George Bouras^{1,2,3}  |
 Roshan Nepal^{1,2,3}  | Ghais Houtak^{1,2,3}  |
 Beula Subashini Panchatcharam^{1,2,3}  | Kevin Aaron Fenix^{1,2,3}  |
 Alkis James Psaltis^{1,2,3}  | Peter-John Wormald^{1,2,3} | Sarah Vreugde^{1,2,3} 

¹Adelaide Medical School, Faculty of Health and Medical Sciences, The University of Adelaide, Adelaide, Australia

²The Department of Surgery-Otolaryngology, Head and Neck Surgery, University of Adelaide, Adelaide, Australia

³The Department of Surgery-Otolaryngology, Head and Neck Surgery, The Basil Hetzel Institute for Translational Health Research, Woodville South, Australia

Correspondence

Sarah Vreugde, Department of Surgery-Otolaryngology, Head and Neck Surgery, University of Adelaide, Adelaide, South Australia, Australia.
 Email: sarah.vreugde@adelaide.edu.au

Funding information

National Health and Medical Research Council, Grant/Award Number: APP1196832; The Garnett Passe and Rodney Williams Memorial Foundation; The Hospital Research Foundation Postgraduate Research Scholarship; The University of Adelaide Scholarship

Abstract

Chronic rhinosinusitis (CRS) represents chronic inflammation of the sinus mucosa characterised by dysfunction of the sinuses' natural defence mechanisms and induction of different inflammatory pathways ranging from a Th1 to a Th2 predominant polarisation. Recalcitrant CRS is associated with *Staphylococcus aureus* dominant mucosal biofilms; however, *S. aureus* colonisation of the sinonasal mucosa has also been observed in healthy individuals challenging the significance of *S. aureus* in CRS pathogenesis. We aimed to investigate the relationship between CRS key inflammatory markers, *S. aureus* biofilm properties/virulence genes and the severity of the disease. Tissue samples were collected during endoscopic sinus surgery from the ethmoid sinuses of CRS patients with (CRSwNP) and without (CRSSNP) nasal polyps and controls ($n = 59$). CD3⁺ T-cell subset frequencies and key inflammatory markers of CD4⁺ helper T cells were determined using FACS analysis. Sinonasal *S. aureus* clinical isolates were isolated ($n = 26$), sequenced and grown into biofilm in vitro, followed by determining their properties, including metabolic activity, biomass, colony-forming units and exoprotein production. Disease severity was assessed using Lund–Mackay radiologic scores, Lund–Kennedy endoscopic scores and SNOT22 quality of life scores. Our results showed that *S. aureus* biofilm properties and CRS severity scores correlated positively with total CD4⁺ T-cell frequencies but looking into CD4⁺ T-cell subsets showed an inverse correlation with Th1 and Th17 cell frequencies. CD4⁺ T-cell frequencies were higher in patients harbouring *lukF.PV*-positive *S. aureus* while its regulatory and Th17 cell subset frequencies were lower in patients carrying *sea*– and *sarT/U*-positive *S. aureus*. Recalcitrant CRS is characterised by increased *S. aureus* biofilm properties in relation to increased total CD4⁺ helper T-cell frequencies and reduced frequencies of its Th1, Th17 and regulatory T-cell

This is an open access article under the terms of the [Creative Commons Attribution](https://creativecommons.org/licenses/by/4.0/) License, which permits use, distribution and reproduction in any medium, provided the original work is properly cited.

© 2023 The Authors. *Immunology* published by John Wiley & Sons Ltd.

subsets. These findings offer insights into the pathophysiology of CRS and could lead to the development of more targeted therapies.

KEYWORDS

CD4+ helper T-cell, Chronic rhinosinusitis, regulatory T cells, *S. aureus* biofilm, sea

INTRODUCTION

Chronic rhinosinusitis (CRS) is a persistent inflammation of the nasal cavity and paranasal sinuses that afflicts up to 10% of the general population, imposing a substantial direct and indirect burden on healthcare systems and economies worldwide [1, 2]. In contrast to the conventional phenotypic classification of CRS into those with (CRSwNP) and without (CRSSNP) nasal polyps [3], endotyping defines the disease variants by their pathophysiologic mechanisms [4].

CRS endotypes are commonly described based on patterns of inflammatory cells, specifically CD4+ T helper (Th) cells which regulate the expression of various chemokines and cytokines. Endotypes of CRS mainly fall into two categories: type 2 (Th2) and non-type 2 (Th1 and Th17) [1]. Th2 is associated with CRSwNP in Caucasian patients and enhanced secretion of IL-4, IL-5, IL-13, IgE antibodies and tissue eosinophilia [3, 5, 6]. Non-Th2 is associated with CRSSNP, but recent studies have shown geographical variation [7, 8]. Th1 is predominantly characterised by increased neutrophils linked to myeloperoxidase and elevated secretion of IFN- γ , IL-2 and TNF- α . Th17 is mainly dominant in Asian patients with CRSwNP and is associated with increased expression of IL-17 and IL-22 cytokines [5]. However, patients do not always fit neatly into these endotypes, making classification difficult [9]. Diverse T-cell polarisations affect the choice of treatment strategies for CRS [10, 11]. Furthermore, regulatory T cells (Tregs) are a specialised subpopulation of T cells that suppress the immune response, maintain homeostasis and self-tolerance and prevent autoimmune disease. The immunosuppressive properties of Tregs are achieved by downregulating effector T cells [12]. The FoxP3 transcription factor is generally used as a marker for identifying these cells [13].

Despite appropriate medical therapy and surgical intervention, 10% of CRS patients suffer from recalcitrant disease. Those patients commonly have nasal polyps with eosinophilia, *Staphylococcus aureus* dominant mucosal biofilms, comorbid asthma and a severely compromised quality of life [14–17]. The remarkable success of *S. aureus* as a pathogen might be due to its numerous measures to protect itself against the host's immune system, including the biofilm mode of existence. Bacteria in biofilms express different genes and proteins from their planktonic counterparts [18, 19] and are more resistant to antimicrobial therapy and host defences [20].

Despite the vast knowledge of inflammatory endotypes in CRS and the significance of *S. aureus* biofilm in this disease, little is known about the relationship between CRS inflammatory markers, *S. aureus* biofilm properties and the severity of the disease. Here, *S. aureus* was isolated from CRS patients and non-CRS controls, grew into biofilm in vitro, and its biofilm properties were characterised in relation to inflammation and CRS severity. We further investigated the relationship between *S. aureus* virulence genes and inflammatory markers in patients' sinonasal tissue. A better understanding of *S. aureus* biofilm properties and their contribution to CRS pathogenesis will be critical for enhancing the prognosis of patients suffering from CRS.

METHODS

Patients and clinical data

Ethics approval for the collection, storage and use of clinical isolates and patient samples from CRS and non-CRS control patients was granted by The Queen Elizabeth Hospital (TQEH) Human Research Ethics Committee, South Australia (HREC/15/TQEH/132), and all patients had signed written informed consent. A prospective study was conducted from 2019 to 2020 with patients recruited from the Queen Elizabeth Hospital, Memorial Hospital and Calvary Hospital, Adelaide, Australia. The diagnostic criteria for CRSwNP and CRSSNP were contented by the American Academy of Otolaryngology and Head and Neck Surgery and the European Position Statement on CRS [15]. Eligibility for the study included age ≥ 18 years and having CRS requiring endoscopic sinus surgery (ESS). The control subjects underwent endoscopic skull base surgery or septoplasty with no clinical or radiologic evidence of sinus disease. Exclusion criteria included using antibiotics or oral corticosteroids the month before surgery. The severity of CRS was measured based on the completion of the Lund–Mackay (LM) [21], Lund–Kennedy (LK) [22, 23] and patient-reported 22-item Sino–Nasal Outcome Test (SNOT-22) questionnaire [24]. A self-reported questionnaire was used to assess the status of asthma, aspirin sensitivity, gastro-oesophageal reflux disease and diabetes mellitus. Sinonasal polyp or mucosal tissue samples were collected from the ethmoid sinuses of CRS patients and the ethmoid sinuses and

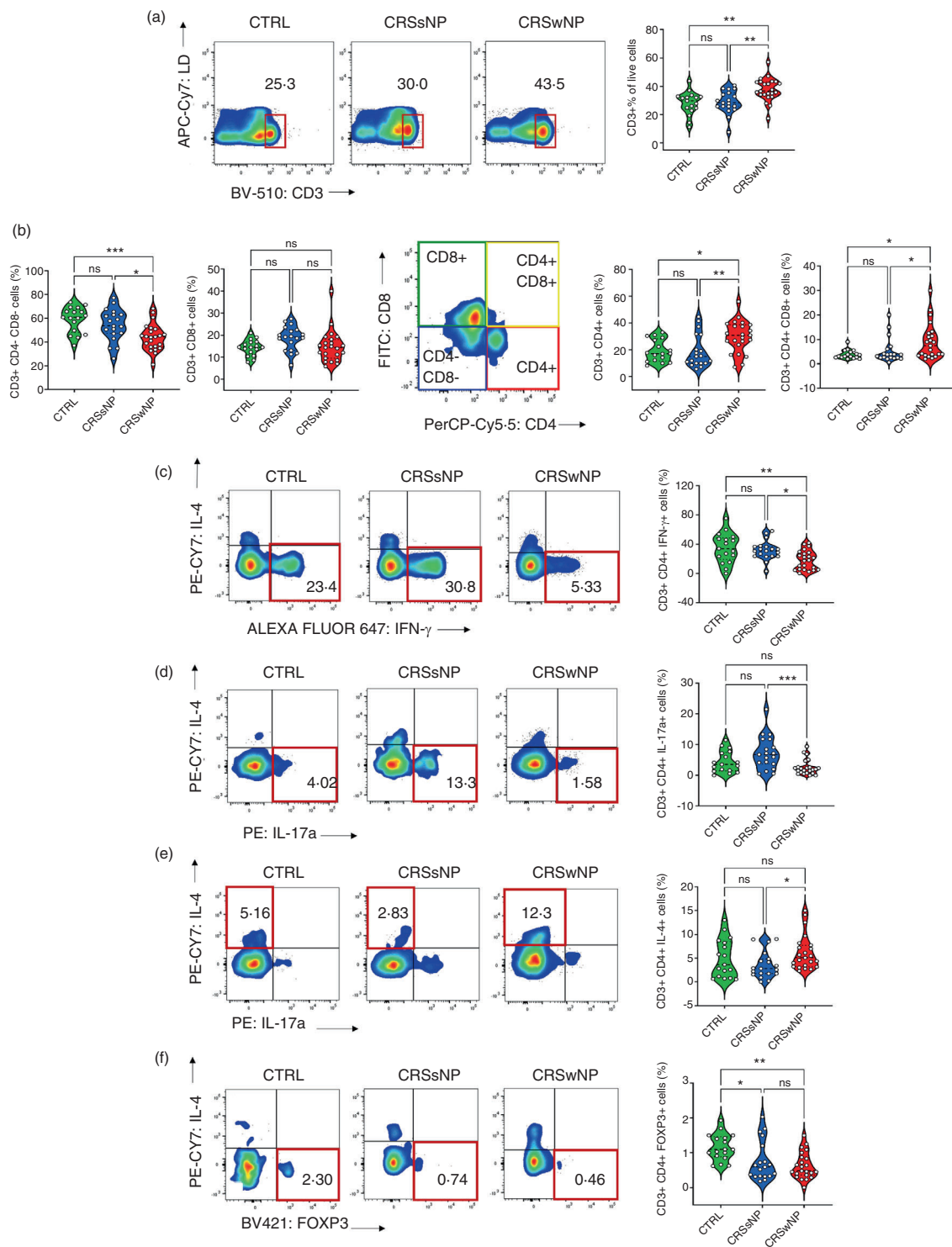


FIGURE 1 The frequency of T-cell subsets in sinonasal tissue of CRS patients and controls. Frequency values for each cell type are displayed in representative flow cytometry plots. The violin plots are displayed as median (dashed line) plus lower and upper quartiles (dotted lines) for CRSwNP ($n = 23$), CRSsNP ($n = 19$) and non-CRS control (CTRL) tissue samples ($n = 17$). The frequency of CD3+ T lymphocytes (a), CD4+ T helper cells, CD8+ T cytotoxic cells, CD4+ CD8+ and CD4- CD8- cells (b), inflammatory markers of Th1 (IFN- γ) (c), Th17 (IL-17a) (d), Th2 (IL-4) (e) and immunosuppressive marker of CD4+ T helper cells (FOXP3) (f). One-way ANOVA followed by Tukey's multiple comparisons test was used, except for CD4+ CD8+ and CD4+ IL-4+ for which Kruskal-Wallis test, followed by Dunn's multiple comparisons test, was used. CRS, chronic rhinosinusitis; CRSsNP, CRS patients without nasal polyps; CRSwNP, CRS patients with nasal polyps.

middle turbinate of non-CRS control subjects during ESS. Nasal swabs were also collected from patients' middle meatus. All samples were immediately transported to the laboratory for processing.

FACS analysis

Fresh sinonasal polyps or mucosal samples were processed into single-cell suspension by enzymatic digestion. For cell surface and intracellular staining, the single-cell suspensions (4×10^6 cells/mL) were stimulated for 4 h at 37°C. Subsequently, the cells were stained with Fixable Viability Dye eFluor[®] 780 (BD Bioscience). Next, the cells were incubated with Fc Block (BD Bioscience) and fluorochrome-conjugated surface antibodies. True-Nuclear Transcription Factor Buffer Set (Biolegend) was used according to the manufacturer's protocol. The cells were then stained with fluorochrome-conjugated intracellular antibodies. Finally, the cells were washed and resuspended in autoMACS Running Buffer (Milteny Biotec, Germany). Multi-colour flow cytometry was performed using a BD FACS Canto II instrument (BD bioscience) and FACS Diva software (BD Bioscience). For each sample, at least 500 000 events were collected. Data were analysed using Flowjo software (FlowJo LLC, Ashland, USA). A summary of immune T cells analysed, and reagents used for FACS is illustrated in Tables S1 and S2.

Isolation of *S. aureus*

Clinical isolates of *S. aureus* were isolated from the nasal swabs of CRS patients and control subjects using mannitol salt agar plates (Oxoid, Basingstoke, UK). The species-level identification was performed using the API Staph (bioMérieux, Australia) and Staphylase test (Oxoid) kits. The isolates were screened for MRSA using a super sensitive and specific chromogenic MRSA selective agar (CHROMID[®] MRSA SMART, bioMérieux, Australia). The *S. aureus* isolates were stored at -80°C in tryptone soy broth (TSB, Oxoid) plus 20% (v/v) sterile glycerol until further analysis.

Evaluation of *S. aureus* biofilm properties

S. aureus biofilm formation

Overnight cultures of *S. aureus* isolates grown on tryptic soy agar (TSA) plates were transferred into a sterile glass tube of 0.9% sodium chloride and adjusted to 1.0 ± 0.1 McFarland turbidity standard (approximately 3×10^8 colony-forming units [CFU]/mL). Next, the bacterial suspension was diluted into the nutrient broth at 1:15 ratio, and 150 μ L of the final

suspension was transferred to flat-bottom 96-well microtiter plates and incubated at 37°C for 48 h in the dark on a gyratory mixer (3D Gyratory Mixer; Ratek Instruments, Boronia, Australia) at 70 rpm to form biofilms.

Evaluation of *S. aureus* biofilm metabolic activity

The metabolic activity of *S. aureus* biofilms was evaluated using an alamarBlue (Resazurin [7-Hydroxy-3H-phenoxazin-3-one10-oxide]) assay. Briefly, 48-h biofilms in black 96-well plates were washed twice with PBS to remove planktonic cells and air-dried for 10 min. The wells were then stained with 200 μ L of 10-fold dilutions of alamarBlue (Invitrogen, Thermo Fisher Scientific, USA) in nutrient broth. Subsequently, the plates were incubated at 37°C on a gyratory mixer in the dark. The wells containing nutrient broth without bacterial culture were considered a sterility control. The fluorescence intensity was then measured at different time points starting from 30 min and followed by 1, 2, 3, 4 and 5 h using the FLUOstar OPTIMA microplate reader (BMG LABTECH, Ortenberg, Germany) at an excitation wavelength of 530 nm and emission of 590 nm until maximum fluorescence was reached. The experiment was performed three times in six replicates. ATCC 25923 was used as a biofilm-forming reference strain of *S. aureus*. The values of *S. aureus* fluorescent intensities were normalised to values for ATCC 25923 and reported as normalised fluorescence intensity.

Evaluation of *S. aureus* biofilm biomass

Forty-eight-hour biofilms in clear 96-well plates were washed with PBS, air-dried and stained with 180 μ L of 0.1% (v/v) crystal violet solution per well for 15 min. Subsequently, the crystal violet was removed, and the plates were rinsed three times with sterile Milli-Q water. Next, 180 μ L/well of 30% acetic acid was added and incubated on a plate shaker until the crystal violet was solubilised. The absorbance was measured at 595 nm using the FLUOstar OPTIMA microplate reader (BMG LABTECH). A sterility control containing uninoculated nutrient broth was used to determine the background optical density. The experiment was performed three times in six replicates. The values of *S. aureus* optical densities were normalised to values for ATCC 25923 and reported as normalised optical densities.

Evaluation of *S. aureus* biofilm CFU

Forty-eight-hour biofilms in 6-well cell plates were washed with PBS. Subsequently, 1 mL of PBS was added to each

well and resuspended thoroughly by pipetting for 3 min to detach the biofilm. Ten-fold serial dilutions of the liquid bacterial cultures were prepared and spot-plated onto TSA plates in $3 \times 20 \mu\text{L}$ spots. The plate was then incubated overnight. The dilutions which gave easy-to-count colonies were selected to count the number of colonies in all three spots. Finally, CFU/mL were calculated using $\text{CFU/mL} = \text{the average number of colonies} \times 50 \times \text{dilution factor}$. The values of *S. aureus* CFU were normalised to values for the ATCC 25923 strain and reported as normalised CFU.

Collection and quantification of *S. aureus* exoprotein

The 48-h *S. aureus* biofilm supernatants from 6-well cell culture plates were collected and centrifuged at $1500 \times g$ for 10 min at 4°C . The clear supernatant was then passed through a $0.22\text{-}\mu\text{m}$ acrodisc[®] syringe filter (Life science, Fribourg, Switzerland). *S. aureus* exoprotein concentrations were then measured using the Nano orange protein quantitation kit (Molecular Probes, Eugene, OR, USA) according to the manufacturer's instructions. The fluorescence intensity was measured with excitation at 485 nm and emission at 590 nm using the FLUOstar Optima (BMG Lab Tech) microplate reader.

DNA extraction and whole-genome sequencing of *S. aureus* clinical isolates

DNA extraction and whole-genome sequencing (WGS) were performed by SA Pathology, Adelaide, Australia. In brief, *S. aureus* isolates were grown on nutrient agar plates (Sigma-Aldrich) at 37°C overnight. Genomic DNA was then extracted using the MN NucleoSpin[®] Microbial DNA extraction kit (Machery-Nagel GmbH and Co.KG, Duren, Germany). Sequencing libraries were prepared using a modified protocol for the Nextera XT DNA library preparation kit (Illumina Inc., San Diego, CA, USA). Briefly, genomic DNA was fragmented, followed by the amplification of Nextera XT indices (Illumina Inc.) to the DNA fragments using a low-cycle PCR reaction. Subsequently, the amplicon library was manually purified and normalised. Sequencing was performed on the Illumina NextSeq 550 platform with NextSeq 500/550 Mid-Output kit v 2.5 (Illumina Inc.), yielding paired-end 150 bp reads. Quality control on sequencing reads was conducted using FastQC (v 0.11.9) [25].

Genomic analysis

S. aureus genomes were assembled using Unicycler v 0.4.8 [26] and annotated with Prokka v 1.14.6 [27].

Assemblies were quality-controlled using QUAST, v 5.0.2 [28]. All genomes were MLST typed and grouped into Clonal Complexes using the MLST [29] (<https://github.com/tseemann/mlst>). Antimicrobial resistance and virulence genes were identified by screening all isolate contigs through the Comprehensive Antibiotic Resistance Database (<https://card.mcmaster.ca/>) and Virulence Factor Database (<https://card.mcmaster.ca/>) using ABRicate, v 1.0.1 (<https://github.com/tseemann/abricate>).

Statistical analysis

Statistical calculations were performed using Graph Pad Prism v 9.0.0 (121) (GraphPad Software, San Diego CA, USA). Statistical differences among groups were evaluated using one-way ANOVA or Kruskal–Wallis test depending on the normality of the variables' distribution. The Independent Samples *t*-test was used to assess the statistical differences between the means of two groups. The Pearson or Spearman's rank correlation coefficient was used for the correlation analysis where *r*-value: 0.00–0.19 = very weak, 0.20–0.39 = weak, 0.40–0.59 = moderate, 0.60–0.79 = strong and 0.80–1.0 = very strong. The results were considered statistically significant when the *p*-value was < 0.05 . * $p < 0.05$; ** $p < 0.01$; *** $p < 0.001$ and **** $p < 0.0001$.

RESULTS

Demographic data and clinical details

A total of 63 participants were recruited for this study. They included CRSwNP ($n = 25$) with a mean age of 56.16 years (range 30–75) and 14/10 male/female ratio (56.00% male); CRSsNP ($n = 21$) with a mean age of 55.81 years (range 19–83) and 14/7 male/female ratio (66.67% male) and non-CRS controls ($n = 17$) with a mean age of 47.29 years (range 20–77) and 8/9 male/female ratio (47.06% male). Of all CRSwNP patients, 72.00% (18/25) had asthma, while only 14.29% (3/21) of CRSsNP patients and 11.76% (2/17) of controls had asthma. 24.00% (6/25) of patients with CRSwNP had aspirin sensitivity, while it was only reported in 4.76% (1/21) of CRSsNP patients and none of the non-CRS controls. The demographic data and clinical characteristics of patients are detailed in Table S3. The severity of CRS disease in CRSwNP, CRSsNP and control subjects is illustrated in Figure S1.

Th1 and Th17 cell frequencies are elevated in CRSsNP, Th2 cell frequencies are elevated in CRSwNP, but Treg frequencies are decreased in both groups compared to control

The flow cytometric analysis of fresh sinonasal polyp or mucosal samples from CRSwNP ($n = 23$), CRSsNP ($n = 19$) and non-CRS control subjects ($n = 17$) was conducted, and a multiparametric flow cytometry approach was applied for the gating strategy, detailed in Figure S2. Our results showed a significant increase in the frequency of total T lymphocytes (CD3+) in CRSwNP compared to CRSsNP ($p = 0.0025$) and controls ($p = 0.0012$; Figure 1a). Four subpopulations of CD3+ T cells, including helper T cells (CD4+), cytotoxic T cells (CD8+), double-positive CD4 and CD8 (CD4+CD8+) and double-negative CD4 and CD8 (CD4-CD8-) were also evaluated. The frequency of CD4+ cells was increased in CRSwNP patients' tissue compared to CRSsNP ($p = 0.0065$) and controls ($p = 0.0106$). A significant increase was also found in the frequency of CD4+CD8+ cells in CRSwNP compared to CRSsNP ($p = 0.0451$) and controls ($p = 0.0239$). No significant changes were observed in CD8+ cytotoxic T-cell frequencies among the patient cohorts ($p > 0.05$). In contrast, there was a significant decrease in CD4-CD8- cell frequencies in CRSwNP compared to CRSsNP ($p = 0.0223$) and controls ($p = 0.0008$; Figure 1b). The quantification of key inflammatory markers of helper T cells, including Th1 (CD4+ IFN- γ), Th2 (CD4+ IL-4+) and Th17 (CD4+ IL-17a+) and Tregs (CD4+ FOXP3+) indicated a significant reduction in the frequencies of Th1 cells in CRSwNP compared to CRSsNP ($p = 0.0189$) and controls ($p = 0.0039$), a reduction in Th17 cells in CRSwNP compared to CRSsNP ($p = 0.0008$) and a reduction in Tregs in both CRSsNP ($p = 0.0250$)

and CRSwNP ($p = 0.0013$) compared to controls. In contrast, there was a significant increase in Th2 cells in CRSwNP compared to CRSsNP ($p = 0.0388$; Figure 1c-f). The frequency of cytotoxic T lymphocytes Tc1 (CD8+ IFN- γ +) was reduced in CRSwNP compared to CRSsNP, while the frequency of CD8+ FOXP3+ T cells was reduced in CRSwNP compared to the control. Results of CD8+ cytotoxic T cells (Tc) expressing IFN- γ +, IL-4+, IL-17a+ and FOXP3+ are shown in Figure S3. The frequency of CD3+ IFN- γ + cells was decreased in CRSwNP compared to CRSsNP and controls, but no significant differences were observed in CD3+ IL-4+, CD3+ IL-17a+ and CD3+ FOXP3+ cell frequencies among patient cohorts (Figure S4).

CRSwNP patients have higher Th2/Th1 and Th2/Th17 ratios than CRSsNPs

Th2/Th1, Th2/Th17 and Th1/Th17 ratios analysis between CRSwNP ($n = 23$), CRSsNP ($n = 19$) and non-CRS control ($n = 17$) showed a higher Th2/Th1 (IL-4/IFN- γ) ratio in CRSwNP compared to CRSsNP ($p = 0.0015$) and controls ($p = 0.0416$) and a higher Th2/Th17 (IL-4/IL-17a) ratio in CRSwNP compared to CRSsNP ($p = 0.0002$). No significant differences were observed in the Th1/Th17 ratio among the patient cohorts ($p > 0.05$; Figure 2).

S. aureus is almost equally distributed between CRS and control patients

From 63 CRS patients and controls, 26 (~42%) *S. aureus* and MRSA isolates were identified. These included 18/46 (39.13%) from CRS patients (9/25 from CRSwNP and

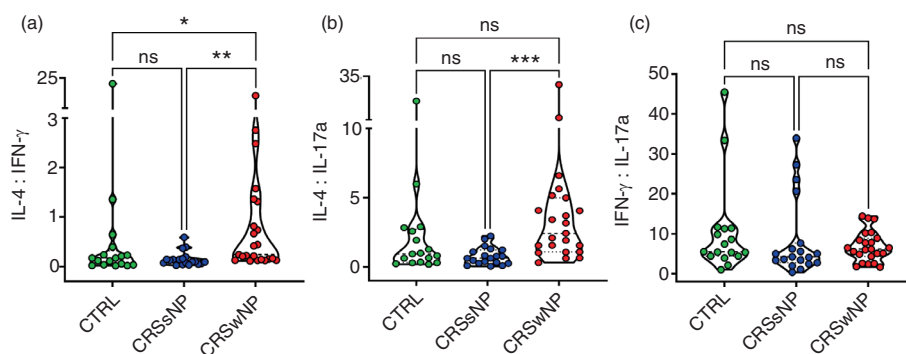


FIGURE 2 The ratio analysis of Th2/Th1 (a), Th2/Th17 (b), and Th1/Th17 (c) between CRSwNP (red dots, $n = 23$), CRSsNP (blue dots, $n = 19$) and non-CRS control (CTRL) tissue samples (green dots, $n = 17$). Kruskal–Wallis test, followed by Dunn's multiple comparisons test, was used. CRS, chronic rhinosinusitis; CRSsNP, CRS patients without nasal polyps; CRSwNP, CRS patients with nasal polyps.

	Samples	<i>S. aureus</i> +	<i>S. aureus</i> -
CTRL	17	8	9
CRSsNP	21	9	12
CRSwNP	25	9	16
Total	63	26	37

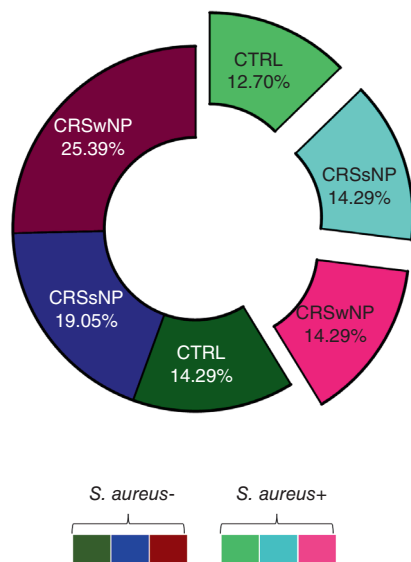


FIGURE 3 The number and distribution of *Staphylococcus aureus*+ and *S. aureus*- in CRSwNP, CRSsNP and non-CRS control patients. CRS, chronic rhinosinusitis; CRSsNP, CRS patients without nasal polyps; CRSwNP, CRS patients with nasal polyps.

9/21 from CRSsNP) and 8/17 (47.05%) from controls (Figure 3). Of all *S. aureus* clinical isolates, 20 were MSSA, whereas 6 isolates were MRSA. The characteristics of *S. aureus* and MRSA isolates are detailed in Table S4.

***S. aureus* from CRSwNP is characterised by high metabolic activity, high biomass, high exoprotein production and high CFU counts**

In vitro-grown *S. aureus* biofilm properties such as metabolic activity, biomass, exoprotein production and CFU were evaluated. As shown in Figure S5, the metabolic activity was variable among different isolates at different time points, but the highest variability was observed at 1 h after incubation with alamarBlue. The quantification of *S. aureus* biofilm metabolic activity in the patient cohorts showed higher metabolic activity in CRSwNP-derived clinical isolates than those from CRSsNP ($p = 0.0010$) and controls ($p = 0.0012$) at 1 h after incubation with alamarBlue (Figure 4a). In addition, CRSwNP-derived *S. aureus* biofilms showed

higher biomass compared to CRSsNP ($p = 0.0073$) and controls ($p = 0.0276$; Figure 4b). Higher CFU/mL were also detected in *S. aureus* biofilms derived from CRSwNP patients than those from controls ($p = 0.0431$; Figure 4c). Furthermore, the CRSwNP-derived clinical isolates exhibited higher exoprotein production than CRSsNP-derived clinical isolates ($p = 0.0241$; Figure 4d).

CRS severity scores correlate positively with CD4+ and CD4+CD8+ T-cell frequencies, but inversely with Th1, Th17 and Tregs

Spearman rank correlation coefficient was calculated to determine whether CRS patients' severity scores and the frequency of T-cell subsets and T helper inflammatory cytokines were related. Weak to moderate positive correlations were observed between CRS severity scores (LM, LK and SNOT22) and the frequencies of CD3+ T cells, CD4+ T cells and CD4+CD8+ T cells (Figure 5a–c). There were inverse correlations between CRS severity scores and the frequencies of CD4–CD8–, Th1 (CD4+ IFN- γ), Th17 (CD4+ IL-17a+) and Tregs (CD4+ FOXP3+; Figure 5d–g).

***S. aureus* biofilm properties correlate positively with CD4+ T-cell frequencies, but inversely with Th1 and Th17 cell frequencies**

The correlation analysis between the in vitro-grown *S. aureus* biofilm properties and the frequency of CD3+ T-cell subsets ($n = 22$) revealed a strong positive correlation between *S. aureus* metabolic activity and the frequency of CD4+ helper T cells ($r = 0.61$, $p = 0.0024$). CD4+ T cells also showed positive correlations with *S. aureus* biofilm biomass ($r = 0.46$, $p = 0.0306$), CFU counts ($r = 0.40$, $p = 0.067$) and exoprotein concentration ($r = 0.38$, $p = 0.077$; Figure 6a). In contrast, moderate inverse correlations were observed between CD4–CD8– T-cell frequencies and *S. aureus* metabolic activity ($r = -0.42$, $p = 0.0498$), CFU counts ($r = -0.45$, $p = 0.0348$) and exoprotein concentration ($r = -0.43$, $p = 0.0467$; Figure 6b). Similarly, *S. aureus* CFU counts and exoprotein concentration exhibited an inverse correlation with Th1 (CD4+ IFN- γ); $r = -0.53$, $p = 0.012$) and Th17 (CD4+ IL-17a+; $r = -0.42$, $p = 0.0496$), respectively (Figure 6c). Furthermore, *S. aureus* biofilm properties were positively correlated with CRS severity scores (Figure S6).

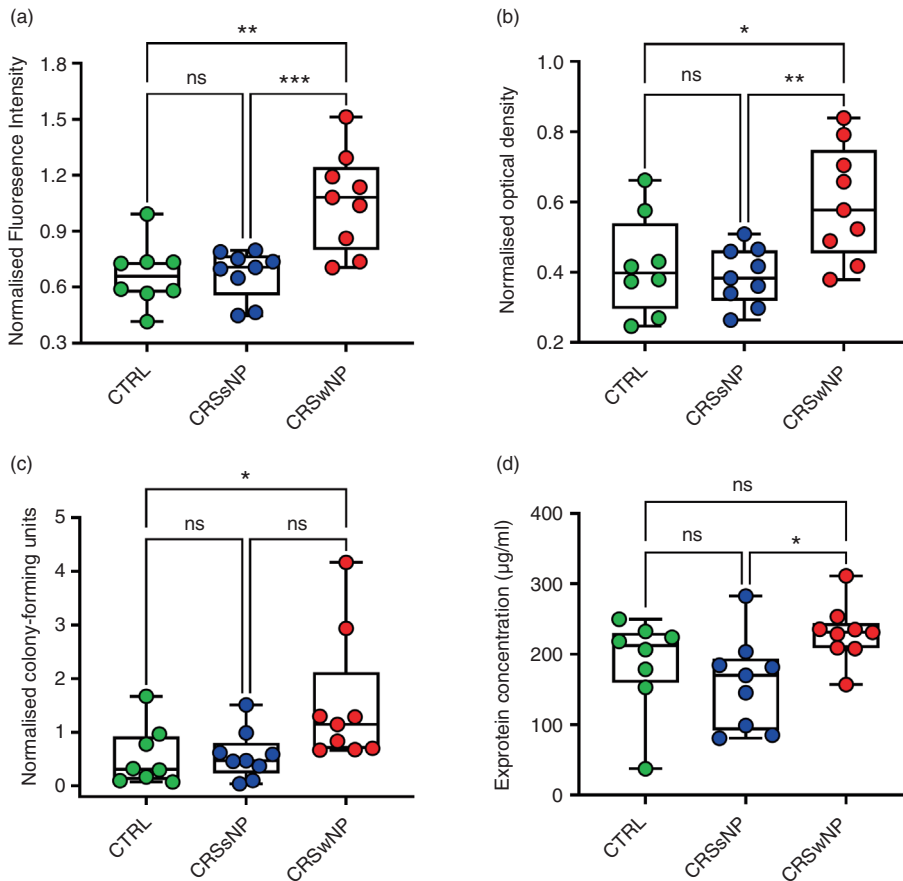


FIGURE 4 The in vitro-grown *Staphylococcus aureus* biofilm metabolic activity, biomass, colony-forming units (CFU) and exoprotein concentration. The normalised fluorescence intensity (a), optical density (b) and CFU (c) represent the *S. aureus* biofilms' metabolic activity at the 1 h time point (a), biomass (b) and CFU/mL (c). *S. aureus* exoprotein concentration ($\mu\text{g}/\text{mL}$) (d). The boxplots are displayed as median plus upper and lower whiskers (the minimum and maximum values) for non-CRS controls (CTRL, green dots, $n = 8$), CRSsNP (blue dots, $n = 9$) and CRSwNP (red dots, $n = 9$). Data were normalised to values for ATCC 25923 (a–c). One-way ANOVA followed by Tukey's multiple comparisons test in (a) and (b), and Kruskal–Wallis test followed by Dunn's multiple comparisons test in (c) and (d) were used. CRS, chronic rhinosinusitis; CRSsNP, CRS patients without nasal polyps; CRSwNP, CRS patients with nasal polyps.

CD4⁺ T-cell frequencies are higher in CRS patients harbouring *lukF.PV*-positive *S. aureus*, while T regulatory and Th17 cell frequencies are lower in CRS patients carrying *sea*- and *sarT/U*-positive *S. aureus*

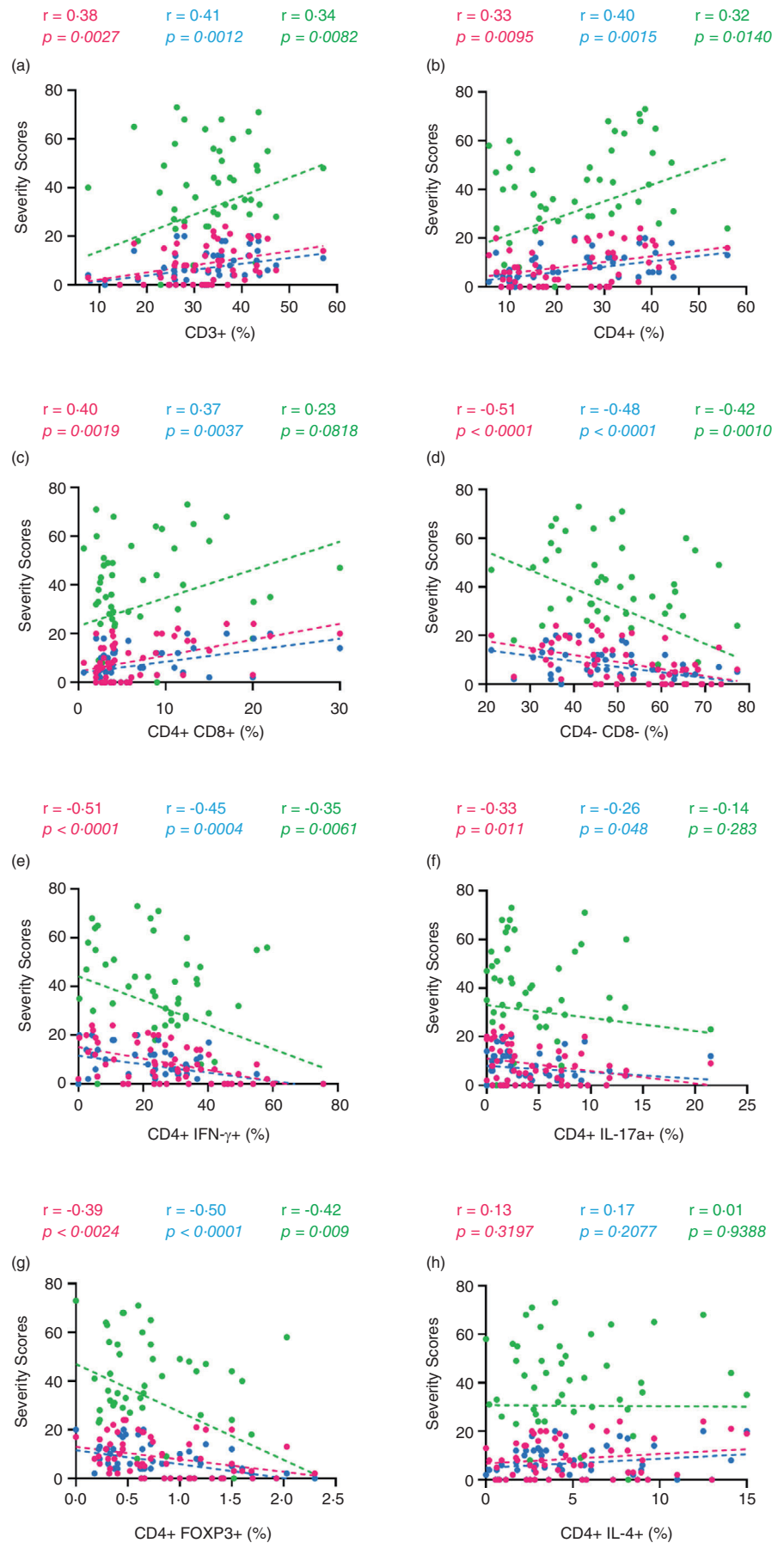
WGS of 26 *S. aureus* isolates derived from CRSwNP, CRSsNP and non-CRS control patients was carried out, and their antimicrobial resistance ($n = 16$) and virulence ($n = 79$) genes were identified. All genomes of *S. aureus* isolates were grouped into the seven most prevalent clonal complexes (CC1, CC15, CC22, CC30, CC45, CC5 and CC8), comprising about ~81% of the isolates. Five isolates had unknown clonal complexes and were classified under 'other'. The presence/absence profile of antimicrobial resistance and virulence genes in different clonal complexes was examined (Figure 7a). The correlation analysis between antimicrobial resistance and virulence genes and T-cell subsets showed higher CD4⁺ helper T-cell frequencies in mucosal tissue and polyp samples harbouring isolates carrying the *lukF.PV* gene ($p = 0.030$). In contrast, Treg (CD4⁺ FOXP3⁺; $p = 0.0493$) and Th17 cell (CD4⁺ IL-17a⁺; $p = 0.0296$) frequencies were significantly lower in samples harbouring isolates carrying the *sea* and *sarT/U* genes,

respectively (Figure 7b). Furthermore, Treg (CD4⁺ FOXP3⁺) frequencies, as well as CD3⁺ and CD4⁺ cell frequencies, were comparable in samples carrying or lacking the *lukF.PV*, *sea* and *fnbA* genes, respectively (Figure S7).

DISCUSSION

This is the first study to show the correlation of CD3⁺ cell subsets in the sinonasal tissue of CRS and non-CRS control patients with CRS severity scores, in vitro-grown biofilm properties and virulence genes of the corresponding patient-derived *S. aureus*. Our results show significant immunophenotypic differences in CD3⁺ cell subsets of CRS patients in relation to CRS disease severity, suggesting that these cells might play a critical role in CRS pathogenesis. Furthermore, the positive correlation of *S. aureus* biofilm properties and virulence genes with CD4⁺ T-cell frequencies and an inverse correlation with Th1 and Th17 cell frequencies, provides a novel understanding of how strain-dependent variation in *S. aureus* biofilm properties and genomic content marks disease severity and relates to immune polarisation.

FIGURE 5 The correlation analysis between chronic rhinosinusitis (CRS) severity scores and the frequency of CD3+ T-cell subsets in the sinonasal tissue from CRS patients and controls ($n = 59$). Each dot represents the result for one patient for the Lund–Mackay radiologic score (pink dots), Lund–Kennedy endoscopic score (blue dots) and SNOT22 (green dots) with the corresponding T-cell markers frequencies. CD3+ T lymphocytes (a), CD4+ helper T cells (b), CD4+ CD8+ (c), CD4– CD8– (d), CD4+ IFN- γ + (e), CD4+ IL-17a+ (f), CD4+ FOXP3+ (g), CD4+ IL-4+ (h). Spearman's rank correlation coefficient was used.



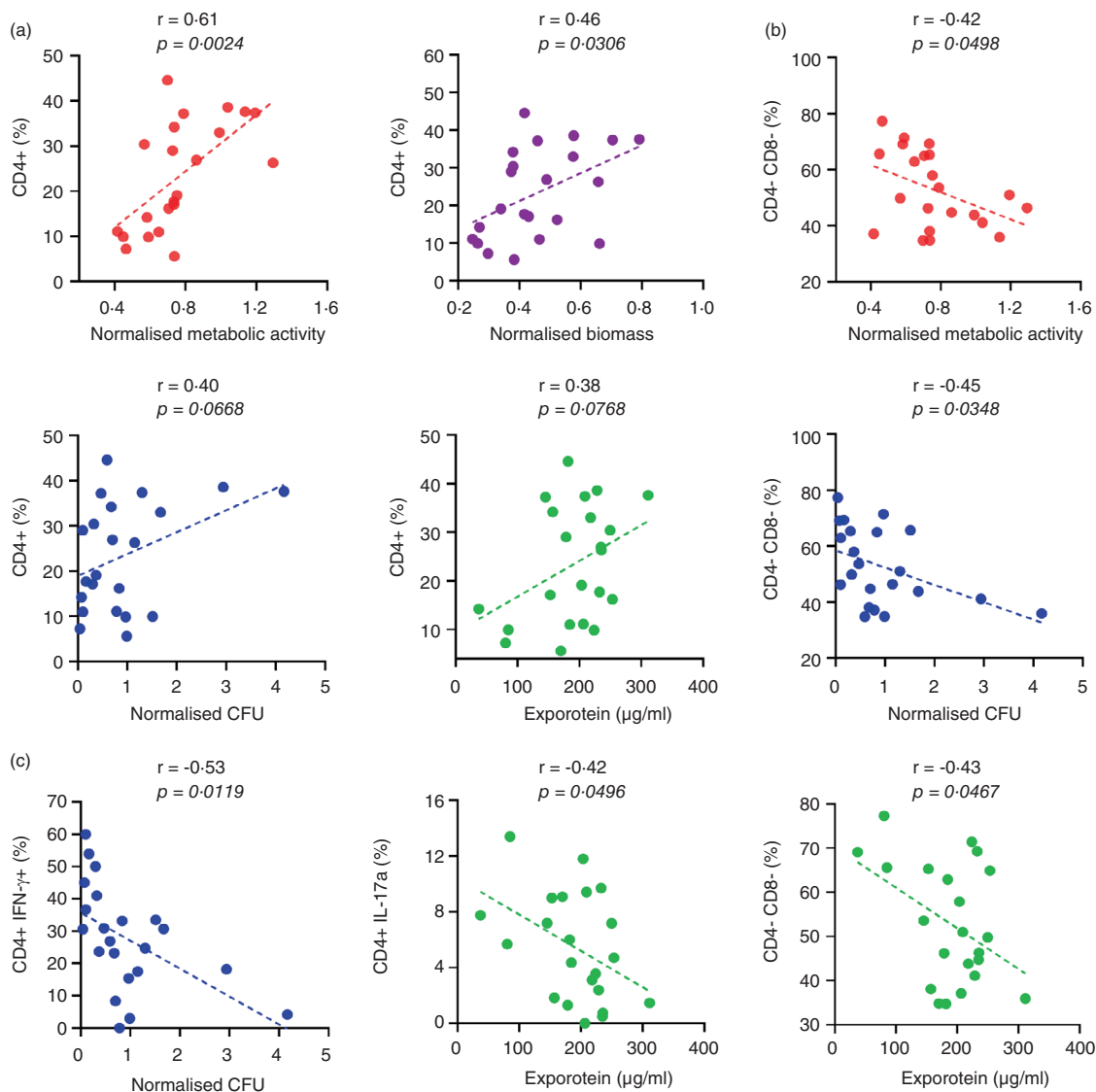
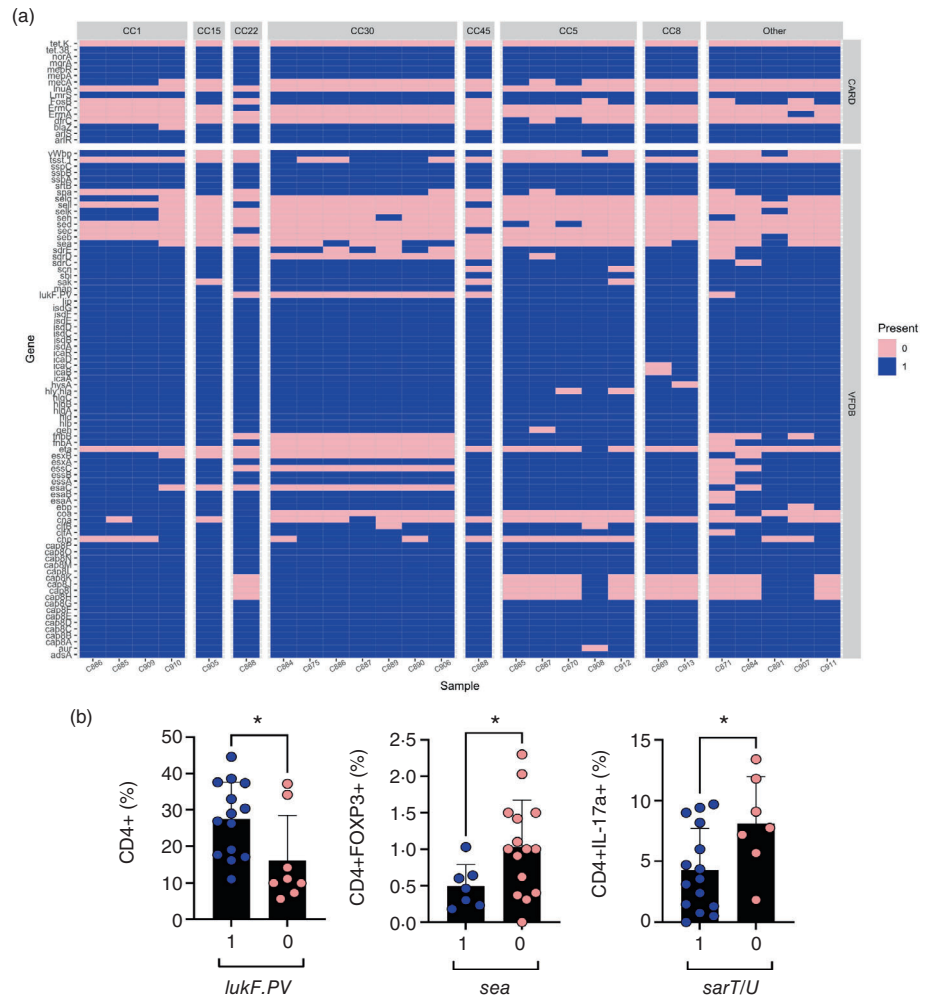


FIGURE 6 The correlation analysis between the in vitro grown *Staphylococcus aureus* biofilm properties and the T-cell subsets frequencies in the sinonasal tissue from chronic rhinosinusitis (CRS) patients and controls ($n = 22$). In the graphs, each dot represents the result for one patient for T-cell markers frequencies and the corresponding *S. aureus* biofilm metabolic activity (red dots), biomass (purple dots), colony-forming units (CFU/mL) (blue dots) and exoprotein (green dots). The upper-left graphs show the correlation between CD4+ T-cell frequencies and the corresponding *S. aureus* biofilm properties (a). The right-hand graphs show the correlation between CD4- CD8- T-cell frequencies and the corresponding *S. aureus* biofilm properties (b). The lower-left graphs exhibit the correlation between CD4+ IFN- γ + and CD4+ IL-17a+ T-cell frequencies and the corresponding *S. aureus* CFU and exoprotein concentration, respectively (c). Pearson's rank correlation coefficient was performed for the correlation analysis.

In the current study, the FACS analysis of CD3+ T-cell subsets and key inflammatory markers of CD4+ helper T cells (Th1, Th2, Th17 and Tregs) and CD8+ cytotoxic T cells (Tc1, Tc2, Tc17 and Tregs) was carried out. Elevated CD4+ T-cell frequencies in CRSwNP patient tissue agree with previous studies supporting the contribution of those cells in CRS pathogenesis [30, 31]. Numerous studies have also reported an increased frequency of CD4+CD8+ double-positive T cells with ageing and in the context of infectious and autoimmune

diseases, as well as cancer [32–35], suggesting a phenotypic profile linked to memory T cells capable of producing cytokines and lytic enzymes. However, their exact role in CRS is yet to be defined. CD4-CD8- double-negative T-cell frequencies were significantly reduced in CRSwNP patients compared to control. These cells have been reported to have a key role in regulating immune responses in the context of transplant rejection, graft-versus-host disease, autoimmune and infectious diseases [36, 37]. It has also been shown that these cells have a

FIGURE 7 The presence/absence profile of 16 *Staphylococcus aureus* genes encoding antimicrobial resistance and 79 genes encoding virulence factors. The rows refer to genes, and the columns refer to *S. aureus* clinical isolates. The blue colour or 1 = gene presence, while the pink colour or 0 = gene absence. CC1, CC15, CC22, CC30, CC45, CC5 and CC8 are the clonal complexes to which most isolates belong. The 'Other' group includes isolates without a defined Clonal Complex (a). CD3+ T-cell subsets frequencies in sinonasal tissue from chronic rhinosinusitis (CRS) patients and non-CRS controls in relation to the presence/absence of patients' *S. aureus* virulence genes (b). The plots are displayed as mean \pm SD, and 1 = gene present and 0 = gene absent in (b). The independent-sample *t*-test was used to compare the groups.



regulatory function similar to Tregs and possess a unique array of cytokines, including IL-4, IL-17 and IFN- γ [38]. However, their function in CRS warrants further investigation.

The higher frequency of Th1 and Th17 cells in CRSsNP and Th2 cells in CRSwNP suggests a non-Th2 skewed inflammation in CRSsNP patients and a Th2 polarisation in our CRSwNP patients. Since these cytokines are not entirely restricted to a specific inflammatory pathway and their ratio determines the ultimate consequence on immune activation [39], their ratio analysis was conducted to confirm the type of inflammation. Higher IL-4/IL-17a (Th2/Th17) and IL-4/IFN- γ (Th2/Th1) in CRSwNP patient tissue demonstrated a Th2-polarised inflammatory milieu in those patients, while higher IFN- γ /IL-4 (Th1/Th2) confirmed Th1 dominance in CRSsNP. Furthermore, decreased Tregs in CRS patients are in line with previous studies [40, 41], suggesting poor recruitment of those cells in CRSwNP [12, 42] potentially due to their impaired migratory function, which ultimately contributes to inflammation [43].

The positive correlation of CD3+, CD4+ and CD4+CD8+ T cells with LM, LK and SNOT22 severity scores in CRS implies that the substantial expansion of those cells might explain the severity of inflammation. In contrast, the inverse correlation of Th1 and Th17 cell frequencies with CRS severity scores suggests the induction of non-Th2 skewed inflammation in mild CRS cases. This is supported by previous findings where Th2-skewed inflammation is mainly observed in severe CRSwNP, often in association with concomitant asthma [44]. The negative correlation of Tregs and CD4-CD8- double-negative T cells, both having regulatory properties, with disease severity, suggests that impaired regulatory function is associated with severe disease in CRS. Those cells might serve as potential biomarkers of disease severity. Interestingly, some inflammatory T cells were closely correlated with *S. aureus* biofilm properties. The moderate to strong correlation of CD4+ cell frequencies with *S. aureus* biofilm metabolic activity, biomass, CFU counts and exoprotein production is strongly suggestive of the greater immunogenicity of high biofilm-producing *S. aureus* that can lead to CD4+ T-cell expansion in

sinonasal tissues/polyps of CRS patients. The inverse correlation of *S. aureus* biofilm properties with Th1, Th17 and CD4–CD8– T-cell frequencies implies that low biofilm-producing *S. aureus* might induce non-Th2 inflammation with impairment of CD4–CD8– cells. By linking the outcome of the correlations, our study supports the hypothesis that high biofilm-producing *S. aureus* might induce a severe disease by skewing the immune response towards a Th2 inflammation.

S. aureus, as a highly successful pathogenic bacterium, produces a wide range of surface components and extracellular products, including toxins and enzymes that contribute to the pathogenesis of infection [45] by promoting tissue adhesion, immune evasion and host cell damage [46]. Here, we demonstrated higher CD4+ T cells in patient tissue harbouring the isolates carrying the *lukF.PV* gene. Pantone–Valentine Leukocidin, as an important leukotoxin, lyses cells of the leukocytic lineage and destroys neutrophils [47], stimulating the release of proinflammatory cytokines, which might favourably dispose the host to resist infection [48]. Previous studies have shown higher levels of IgG antibodies against LukF-PV in CRS patients, indicating that these specific *S. aureus* antigens affect the pathogenesis of CRS [49]. Staphylococcal superantigens, such as enterotoxins (SEA), are highly mitogenic exotoxins that trigger an enormously powerful stimulatory activity for T lymphocytes, leading to a substantial release of T-cell mediators and proinflammatory cytokines [50, 51], intensifying the Th2 response in the tissue and diminishing the immunosuppressive activity of Tregs, which finally leads to inflammation [52]. This is supported by our findings showing the lower Treg frequencies in patient tissue harbouring *sea*-carrying strains. Furthermore, higher Th17 in patient tissue with *sarT/sarU*-lacking strains indicates that non-Th2 skewed inflammation, which is normally observed in mild CRS cases, might occur due to lack of certain virulence genes such as *sarT* and *sarU*. These genes' products regulate the synthesis of cell-surface proteins such as protein A and exoproducts such as hemolysins by controlling the *agr* locus [53].

In conclusion, stratifying CRS patients based on their inflammatory markers in relation to disease severity and *S. aureus* biofilm properties offers insights into a potential pathogenic link between severe disease and bacterial biofilms, which could lead to the development of more targeted therapies.

AUTHOR CONTRIBUTIONS

Sarah Vreugde and Gohar Shaghayegh conceived the study. Gohar Shaghayegh, Clare Cooksley and Sarah Vreugde contributed to the experimental design. Kevin Aaron Fenix assisted with FACS panel design and

analysis. Gohar Shaghayegh conducted the experiments. Gohar Shaghayegh and George Bouras analysed data. Gohar Shaghayegh and Sarah Vreugde drafted the manuscript. Gohar Shaghayegh made the illustration. Sarah Vreugde, Alkis James Psaltis, Peter-John Wormald and Clare Cooksley provided supervision. Roshan Nepal, Ghais Houtak and Beula Subashini Panchatcharam assisted in sample collection. All authors reviewed the manuscript and approved the submission of this work.

ACKNOWLEDGEMENTS

This study was supported by The Hospital Research Foundation (THRF) Postgraduate Research Scholarship and The University of Adelaide scholarship. We thank all the members of the ENT Surgery Group, Basil Hetzel Institute, who directly and indirectly assisted in collecting samples from patients. The illustration was created with [Biorender.com](https://www.biorender.com). Open access publishing facilitated by The University of Adelaide, as part of the Wiley - The University of Adelaide agreement via the Council of Australian University Librarians.

CONFLICT OF INTEREST STATEMENT

All authors declare no conflict of interest.

DATA AVAILABILITY STATEMENT

The data that supports the findings of this study are available in the supplementary material of this article.

ORCID


Gohar Shaghayegh  <https://orcid.org/0000-0002-9822-5392>

Clare Cooksley  <https://orcid.org/0000-0003-3109-4540>

George Bouras  <https://orcid.org/0000-0002-5885-4186>

Roshan Nepal  <https://orcid.org/0000-0002-5469-3397>

Ghais Houtak  <https://orcid.org/0000-0001-6692-9478>

Beula Subashini Panchatcharam  <https://orcid.org/0000-0001-5762-8008>

Kevin Aaron Fenix  <https://orcid.org/0000-0003-1619-1406>

Alkis James Psaltis  <https://orcid.org/0000-0003-2967-1855>

Sarah Vreugde  <https://orcid.org/0000-0003-4719-9785>

REFERENCES

1. Fokkens WJ, Lund VJ, Hopkins C, Hellings PW, Kern R, Reitsma S, et al. European position paper on rhinosinusitis and nasal polyps 2020. *Rhinology*. 2020;58:1–464.
2. Bachert C, Marple B, Schlosser RJ, Hopkins C, Schleimer RP, Lambrecht BN, et al. Adult chronic rhinosinusitis. *Nat Rev Dis Primers*. 2020;6(1):1–19.
3. Bachert C, Akdis CA. Phenotypes and emerging endotypes of chronic rhinosinusitis. *J Allergy Clin Immunol*. 2016;4(4):621–8.
4. Akdis CA, Bachert C, Cingi C, Dykewicz MS, Hellings PW, Naclerio RM, et al. Endotypes and phenotypes of chronic

- rhinosinusitis: a PRACTALL document of the European Academy of Allergy and Clinical Immunology and the American Academy of Allergy, Asthma & Immunology. *J Allergy Clin Immunol*. 2013;131(6):1479–90.
5. Annunziato F, Romagnani C, Romagnani S. The 3 major types of innate and adaptive cell-mediated effector immunity. *J Allergy Clin Immunol*. 2015;135(3):626–35.
 6. Tomassen P, Vandeplas G, Van Zele T, Cardell L-O, Arebro J, Olze H, et al. Inflammatory endotypes of chronic rhinosinusitis based on cluster analysis of biomarkers. *J Allergy Clin Immunol*. 2016;137(5):1449–1456.e4.
 7. Tan BK, Klingler AI, Poposki JA, Stevens WW, Peters AT, Suh LA, et al. Heterogeneous inflammatory patterns in chronic rhinosinusitis without nasal polyps in Chicago, Illinois. *J Allergy Clin Immunol*. 2017;139(2):699–703.
 8. Stevens WW, Ocampo CJ, Berdnikovs S, Sakashita M, Mahdavinia M, Suh L, et al. Cytokines in chronic rhinosinusitis: role in eosinophilia and aspirin-exacerbated respiratory disease. *Am J Respir Crit Care Med*. 2015;192(6):682–94.
 9. Stevens WW, Peters AT, Tan BK, Klingler AI, Poposki JA, Hulse KE, et al. Associations between inflammatory endotypes and clinical presentations in chronic rhinosinusitis. *J Allergy Clin Immunol*. 2019;7(8):2812–20.
 10. Van Zele T, Claeys S, Gevaert P, Van Maele G, Holtappels G, Van Cauwenberge P, et al. Differentiation of chronic sinus diseases by measurement of inflammatory mediators. *Allergy*. 2006;61(11):1280–9.
 11. Zhang N, Van Zele T, Perez-Novo C, Van Bruaene N, Holtappels G, DeRuyck N, et al. Different types of T-effector cells orchestrate mucosal inflammation in chronic sinus disease. *J Allergy Clin Immunol*. 2008;122(5):961–8.
 12. Van Bruaene N, Pérez-Novo CA, Basinski TM, Van Zele T, Holtappels G, De Ruyck N, et al. T-cell regulation in chronic paranasal sinus disease. *J Allergy Clin Immunol*. 2008;121(6):1435–41.
 13. Sakaguchi S, Miyara M, Costantino CM, Hafler DA. FOXP3+ regulatory T cells in the human immune system. *Nat Rev Immunol*. 2010;10(7):490–500.
 14. Gall M, Krysiak K, Prescott V. Asthma, chronic obstructive pulmonary disease, and other respiratory diseases in Australia. Canberra, Australia: Australian Institute of Health and Welfare; 2010.
 15. Fokkens WJ, Lund VJ, Mullol J, Bachert C, Alobid I, Baroody F, et al. EPOS 2012: European position paper on rhinosinusitis and nasal polyps 2012. A summary for otorhinolaryngologists. *Rhinology*. 2012;50(1):1–12.
 16. Foreman A, Psaltis AJ, Tan LW, Wormald P-J. Characterization of bacterial and fungal biofilms in chronic rhinosinusitis. *Am J Rhinol Allergy*. 2009;23(6):556–61.
 17. Psaltis AJ, Weitzel EK, Ha KR, Wormald P-J. The effect of bacterial biofilms on post-sinus surgical outcomes. *Am J Rhinol*. 2008;22(1):1–6.
 18. Flemming H-C, Neu TR, Wozniak DJ. The EPS matrix: the “house of biofilm cells”. *J Bacteriol*. 2007;189(22):7945–7.
 19. Gil C, Solano C, Burgui S, Latasa C, García B, Toledo-Arana A, et al. Biofilm matrix exoproteins induce a protective immune response against *Staphylococcus aureus* biofilm infection. *Infect Immun*. 2014;82(3):1017–29.
 20. Singhal D, Psaltis AJ, Foreman A, Wormald P-J. The impact of biofilms on outcomes after endoscopic sinus surgery. *Am J Rhinol Allergy*. 2010;24(3):169–74.
 21. Lund VJ, Mackay IS. Staging in rhinosinusitis. *Rhinology*. 1993;31:183.
 22. Lund VJ, Kennedy DW. Staging for rhinosinusitis. *Otolaryngol Head Neck Surg*. 1997;117(3):S35–40.
 23. Psaltis AJ, Li G, Vaezaefshar R, Cho KS, Hwang PH. Modification of the Lund–Kennedy endoscopic scoring system improves its reliability and correlation with patient-reported outcome measures. *Laryngoscope*. 2014;124(10):2216–23.
 24. Hopkins C, Gillett S, Slack R, Lund V, Browne J. Psychometric validity of the 22-item Sinonasal Outcome Test. *Clin Otolaryngol*. 2009;34(5):447–54.
 25. Andrews S. FastQC: a quality control tool for high throughput sequence data. Babraham bioinformatics. Cambridge: Babraham Institute; 2010.
 26. Wick RR, Judd LM, Gorrie CL, Holt KE. Unicycler: resolving bacterial genome assemblies from short and long sequencing reads. *PLoS Comput Biol*. 2017;13(6):e1005595.
 27. Seemann T. Prokka: rapid prokaryotic genome annotation. *Bioinformatics*. 2014;30(14):2068–9.
 28. Gurevich A, Saveliev V, Vyahhi N, Tesler G. QUAST: quality assessment tool for genome assemblies. *Bioinformatics*. 2013;29(8):1072–5.
 29. Jolley KA, Bray JE, Maiden MC. Open-access bacterial population genomics: BIGSdb software, the PubMLST.org website and their applications. *Wellcome Open Res*. 2018;3:124.
 30. Akdis M, Aab A, Altunbulakli C, Azkur K, Costa RA, Cramer R, et al. Interleukins (from IL-1 to IL-38), interferons, transforming growth factor β , and TNF- α : receptors, functions, and roles in diseases. *J Allergy Clin Immunol*. 2016;138(4):984–1010.
 31. Wherry EJ, Masopust D. Adaptive immunity: neutralizing, eliminating, and remembering for the next time. In: *Viral pathogenesis: from basics to systems biology*. 3rd ed. Elsevier Inc; 2016. p. 57–69. <https://doi.org/10.1016/B978-0-12-800964-2.00005-7>
 32. Overgaard NH, Jung JW, Steptoe RJ, Wells JW. CD4+/CD8+ double-positive T cells: more than just a developmental stage? *J Leukoc Biol*. 2015;97(1):31–8.
 33. Overgaard NH, Cruz JL, Bridge JA, Nel HJ, Frazer IH, la Gruta NL, et al. CD4+ CD8 β + double-positive T cells in skin-draining lymph nodes respond to inflammatory signals from the skin. *J Leukoc Biol*. 2017;102(3):837–44.
 34. Nascimbeni M, Shin E-C, Chiriboga L, Kleiner DE, Rehermann B. Peripheral CD4+ CD8+ T cells are differentiated effector memory cells with antiviral functions. *Blood*. 2004;104(2):478–86.
 35. Nascimbeni M, Pol S, Saunier B. Distinct CD4+ CD8+ double-positive T cells in the blood and liver of patients during chronic hepatitis B and C. *PLoS One*. 2011;6(5):e20145.
 36. Thomson CW, Lee BP-L, Zhang L. Double-negative regulatory T cells. *Immunol Res*. 2006;35(1):163–77.
 37. Villani FNA, da Costa Rocha MO, Nunes MCP, Antonelli LRDV, Magalhaes LMD, dos Santos JSC, et al. Trypanosoma cruzi-induced activation of functionally distinct $\alpha\beta$

- and $\gamma\delta$ CD4⁻ CD8⁻ T cells in individuals with polar forms of Chagas' disease. *Infect Immun*. 2010;78(10):4421–30.
38. Vinton C, Klatt NR, Harris LD, Briant JA, Sanders-Beer BE, Herbert R, et al. CD4-like immunological function by CD4⁻ T cells in multiple natural hosts of simian immunodeficiency virus. *J Virol*. 2011;85(17):8702–8.
 39. Wegrzyn AS, Jakiela B, Rückert B, Jutel M, Akdis M, Sanak M, et al. T-cell regulation during viral and nonviral asthma exacerbations. *J Allergy Clin Immunol*. 2015;136(1):194–197.e9.
 40. Tantilipikorn P, Sookrung N, Muangsomboon S, Lumyongsattien J, Bedavanija A, Suwanwech T. Endotyping of chronic rhinosinusitis with and without polyp using transcription factor analysis. *Front Cell Infect Microbiol*. 2018;8:82.
 41. Seif F, Ghalehbaghi B, Aazami H, Mohebbi A, Ahmadi A, Falak R, et al. Frequency of CD4⁺ and CD8⁺ T cells in Iranian chronic rhinosinusitis patients. *Allergy Asthma Clin Immunol*. 2018;14(1):1–11.
 42. Roongrotwattanasiri K, Pawankar R, Kimura S, Mori S, Nonaka M, Yagi T. Decreased expression of FOXP3 in nasal polyposis. *Allergy Asthma Immunol Res*. 2012;4(1):24–30.
 43. Kim YM, Munoz A, Hwang PH, Nadeau KC. Migration of regulatory T cells toward airway epithelial cells is impaired in chronic rhinosinusitis with nasal polyposis. *Clin Immunol*. 2010;137(1):111–21.
 44. Xu X, Reitsma S, Wang DY, Fokkens WJ. Highlights in the advances of chronic rhinosinusitis. *Allergy*. 2021;76(11):3349–58.
 45. Oliveira D, Borges A, Simões M. *Staphylococcus aureus* toxins and their molecular activity in infectious diseases. *Toxins*. 2018;10(6):252.
 46. Powers ME, Wardenburg JB. Igniting the fire: *Staphylococcus aureus* virulence factors in the pathogenesis of sepsis. *PLoS Pathog*. 2014;10(2):e1003871.
 47. Löffler B, Hussain M, Grundmeier M, Brück M, Holzinger D, Varga G, et al. *Staphylococcus aureus* Panton-Valentine leukocidin is a very potent cytotoxic factor for human neutrophils. *PLoS Pathog*. 2010;6(1):e1000715.
 48. Yoong P, Pier GB. Immune-activating properties of Panton-Valentine leukocidin improve the outcome in a model of methicillin-resistant *Staphylococcus aureus* pneumonia. *Infect Immun*. 2012;80(8):2894–904.
 49. Thunberg U, Hugosson S, Fredlund H, Cao Y, Ehricht R, Monecke S, et al. Anti-Staphylococcal humoral immune response in patients with chronic rhinosinusitis. 2019.
 50. Bachert C, Van Zele T, Gevaert P, De Schrijver L, Van Cauwenberge P. Superantigens and nasal polyps. *Curr Allergy Asthma Rep*. 2003;3(6):523–31.
 51. Heaton T, Mallon D, Venaillie T, Holt P. Staphylococcal enterotoxin induced IL-5 stimulation as a cofactor in the pathogenesis of atopic disease: the hygiene hypothesis in reverse? *Allergy*. 2003;58(3):252–6.
 52. Ou L-S, Goleva E, Hall C, Leung DY. T regulatory cells in atopic dermatitis and subversion of their activity by superantigens. *J Allergy Clin Immunol*. 2004;113(4):756–63.
 53. Cheung AL, Nishina KA, Trotonda MP, Tamber S. The SarA protein family of *Staphylococcus aureus*. *Int J Biochem Cell Biol*. 2008;40(3):355–61.

SUPPORTING INFORMATION

Additional supporting information can be found online in the Supporting Information section at the end of this article.

How to cite this article: Shaghayegh G, Cooksley C, Bouras G, Nepal R, Houtak G, Panchatcharam BS, et al. *Staphylococcus aureus* biofilm properties and chronic rhinosinusitis severity scores correlate positively with total CD4⁺ T-cell frequencies and inversely with its Th1, Th17 and regulatory cell frequencies. *Immunology*. 2023. <https://doi.org/10.1111/imm.13655>